Computations of Vertical Motion and Vorticity Budget in a Blocking Situation

By A. ELIASSEN[1] and W. E. HUBERT[2]
University of Stockholm

(Manuscript received December 2, 1952)

Abstract

The synoptic situation under study is a blocking situation over Western Europe and the North-Eastern Atlantic. Barotropic tendency computations for the 500 mb surface are carried out and compared with the 12 hour observed height change. Tendency computations are also carried out for the mean height (averaged along the vertical with respect to pressure). The vertical motion compatible with the observed local vorticity changes is computed from the vorticity equation at several levels. The result is in fair agreement with the observed distribution of precipitation and cloudiness. The computations indicate that horizontal divergence and horizontal vorticity advection are of about equal importance in the vorticity budget at 500 mb, whereas the vertical vorticity transport seems to be less important.

The equations governing atmospheric motion are very complicated, and the amount of useful information about future development which we have been able to derive from the "exact" equations is certainly small. In recent years, however, one has attempted to overcome the difficulties by a simplified treatment of atmospheric motion, putting the emphasis on the largescale features and neglecting all details. This line of attack has been advocated by ROSSBY, who in 1939 proposed to consider the atmospheric motion as horizontal and non-divergent, so that the motion is characterized by the absolute vertical vorticity being conservative. CHARNEY (1949) has found that this property should be attributed to the motion at a certain "equivalent barotropic level" in the vicinity of the 500 mb level. This very simple "barotropic" model has proved to be very fruitful; it leads to equations which we are able to handle and which explain a considerable part of the observed height changes at the 500 mb surface. On the other hand, it is clear that the barotropic model represents an oversimplification and has severe defects. However, by correcting the model for the more important of these defects, we may hope to arrive at other models that give a more satisfactory description of the observed changes without adding too many complications. From this point of view, it seems to be important to study the errors due to the barotropic model. This is not a very easy undertaking, for the discrepancies of the computed changes are caused not only by the shortcomings of the model itself, but are due to two other sources of errors as well, viz. errors in observation and analysis, and errors which are introduced in the process of numerical integration.

For theoretical reasons, we should expect

[1] On leave of absence from Det Norske Meteorologiske Institutt, Oslo.

[2] Lieutenant, US Navy, from the Office of Naval Research, American Embassy, London.

the barotropic model to be most unsatisfactory in cases of strong development. Another case where the model seems inadequate is in certain quasi-stationary motions. Some exact solutions, representing stationary, horizontal and non-divergent motion on a rotating sphere are known. (CRAIG 1945, HÖILAND 1950). They have the character of waves of finite amplitude with troughs and wedges symmetrical with respect to the meridians. On the other hand, semi-stationary motions with a pronounced tilt of the trough and ridge lines relative to the meridians are often observed. It is difficult to see how such motions could be explained from the conservation of vorticity. An example which frequently occurs in connection with a blocking situation is characterized by an almost zonal flow over the North Atlantic, bending sharply around a cyclone in the vicinity of the British Isles and continuing as a southerly or even southeasterly current towards Iceland and Eastern Greenland. Such a streamline pattern sometimes persists for one or two weeks or more. If we assume that the air particles move horizontally through such a stationary field, we must conclude that their vorticity will increase during the transition from the zonal to the cyclonically curved flow. We should therefore expect important individual vorticity changes to take place in this region.

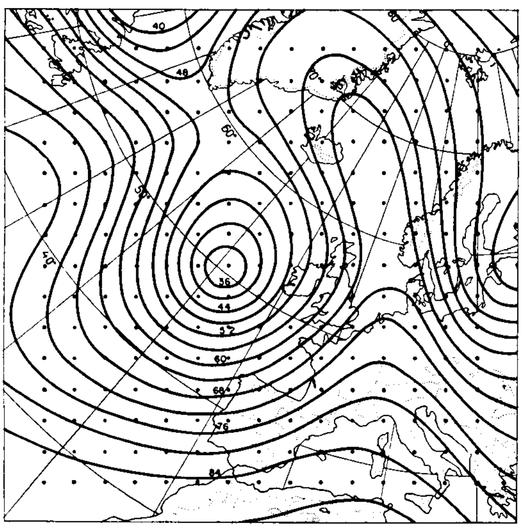

Fig. 1. 500 mb map at 1500 GMT, 24 May 1951 showing the gridpoints used in all calculations. Heights in decameters.

On the basis of such considerations, it was thought that a closer investigation of the vorticity budget in a blocking case might throw some light upon the nature of the deviations from the conservation of vorticity. Through such an investigation, some clarification of the dynamics of the blocking phenomenon might be realized.

Two different courses of action seem to be possible. One might investigate the mean vorticity budget over a longer period by means of maps averaged with respect to time, or on the other hand, the analysis could be based on actual maps. In the former case, the eddy transport of vorticity would enter into the considerations as an important unknown factor. Because of this factor the latter method was chosen. This method, in turn, also presents complications; namely, that the vorticity changes connected with smaller scale wave perturbations that travel through the semi-stationary field will tend to confuse the long-trend effects. However, this difficulty is inevitable since we cannot a priori be certain that these smaller scale motions are not part of the large scale mechanism.

A blocking situation of the type discussed occured from the 19th to the 29th of May, 1951. In its main features, the field of motion over Western Europe and the Eastern Atlantic was almost stationary during this period. The transition from zonal to cyclonic flow took place over the British Isles where the aerological network is good. The twelve hour period from 1500 GMT on the 24th of May to 0300 GMT on the 25th was selected for the study. The 500 mb map at 1500 GMT is shown in Fig. 1.

At first, a tendency computation was performed on the basis of the barotropic model, assuming the local vorticity changes at the 500 mb level to be due to advection only, as expressed by the equation

$$\frac{\partial \zeta}{\partial t} = -\mathbf{v} \cdot \nabla \eta \qquad (1)$$

Here ζ means relative vertical vorticity, t time, $\mathbf{v}$ horizontal wind vector, ∇ horizontal del-operator and η absolute vertical vorticity, which may be written as

$$\eta = \zeta + f \qquad (2)$$

where f is the Coriolis parameter.

When the geostrophic wind approximation is introduced in (1), a Poisson equation for the height tendency results. This equation was treated as described in a report by the STAFF MEMBERS, UNIVERSITY OF STOCKHOLM (1952). Employing a square grid on a conformal map, as shown in Fig. 1, the right-hand side was determined by means of the difference method for the 24th and 25th, and the height tendency was determined by relaxation.

Using a method outlined by BOLIN and CHARNEY (1951), the tendencies thus obtained at the two instants were multiplied by 6 hours and then added to obtain a 12-hour height change. The result is shown in Fig. 2, which was computed under the assumption that the height tendencies along the boundary of the rectangular area were zero. The correlation coefficient between the computed height changes and the observed changes in the same 12-hour period for 49 grid points in the center of the area was 0.84. Fig. 3 shows the computed height changes when the actually observed changes were used as a boundary condition instead of zero values (compare UNIVERSITY OF STOCKHOLM 1952). Somewhat surprisingly, the correlation coefficient between observed and computed changes was only 0.70 in this case. This does not necessarily imply a marked depreciation in the results, but rather demonstrates the inadequacy of judging these tests using correlation coefficients alone. The observed 12-hour height changes of the 500 mb surface are shown in Fig. 4.

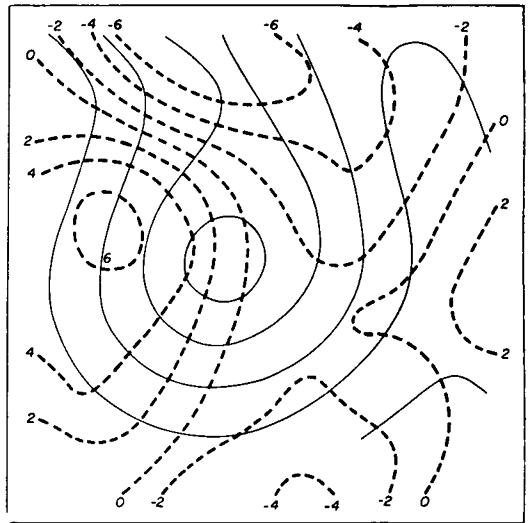

Fig. 3. Computed 500 mb height changes from 1500 GMT, 24 May to 0300 GMT 25 May in decameters. Observed height changes used as a boundary condition.

The figures demonstrate that the computations give rise and fall areas in approximately the correct positions. The most pronounced discrepancy, however, is that the fall area to

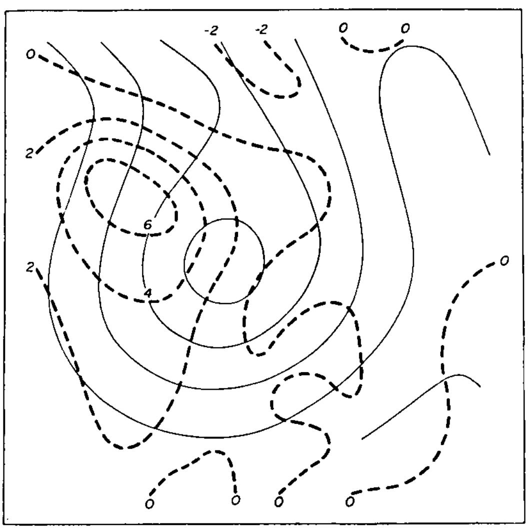

Fig. 2. Computed 500 mb height change from 1500 GMT, 24 May to 0300 GMT 25 May in decameters. Height changes at the boundary assumed to be zero. Mean 500 mb pattern shown by thin solid lines.

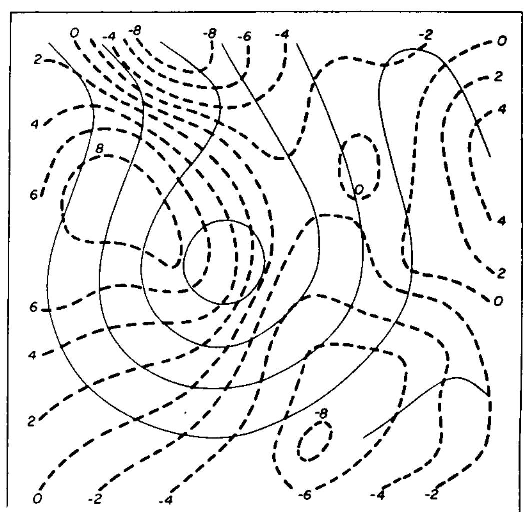

Fig. 4. Observed 500 mb height change from 1500 GMT, 24 May to 0300 GMT, 25 May in decameters.

the SE of the low center is calculated to be too weak. This error is undoubtedly due to the barotropic model; the assumption that local vorticity changes are due to vorticity advection only is too restrictive to give good results in this region.

The "barotropic model" as designed by CHARNEY (1949) was based on the assumption that the vorticity equation averaged in the vertical direction may be written with sufficient accuracy

$$\overline{\frac{\partial \zeta}{\partial t}} + \overline{\mathbf{v} \cdot \nabla (f+\zeta)} = 0 \qquad (3)$$

The application of vorticity conservation to the motion at a certain "equivalent barotropic level", which may be approximately represented by the 500 mb surface, however, rests on certain additional assumptions concerning the variation of wind with height. It is conceivable that the errors are mainly due to these assumptions, and that (3) is a reasonably good approximation. If the wind velocity is sub-divided into a mean wind $\bar{\mathbf{v}}$ and a thermal wind $\mathbf{v}_T$,

$$\mathbf{v} = \bar{\mathbf{v}} + \mathbf{v}_T \qquad \zeta = \bar{\zeta} + \zeta_T \qquad (4)$$

equation (3) may also be written

$$\frac{\partial \bar{\zeta}}{\partial t} = -\bar{\mathbf{v}} \cdot \nabla (f + \bar{\zeta}) - \overline{\mathbf{v}_T \cdot \nabla \zeta_T} \qquad (5)$$

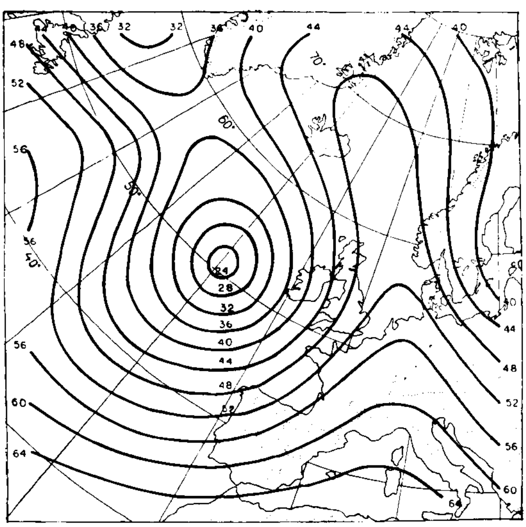

Fig. 5. Mean map for 1500 GMT, 24 May 1951. Isopleths represent ($\bar{z}$ — 700) in decameters.

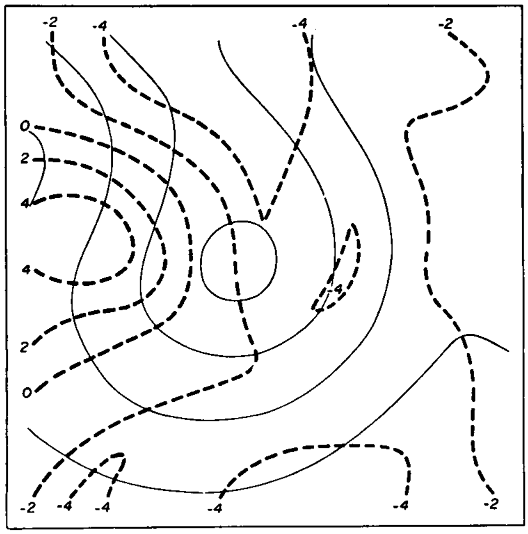

Fig. 6. Computed 12-hour mean height changes from 1500 GMT, 24 May to 0300 GMT, 25 May in decameters. Observed height changes used as a boundary condition. Mean $\bar{z}$ pattern shown by thin solid lines.

When geostrophic winds are used, it is readily seen that $\bar{\mathbf{v}}$ is related to the mean height $\bar{z}$ in the same way as the wind at a particular level is related to the height of the corresponding isobaric surface. Therefore, eq. (5) can be used to determine the local change of the mean height in the same manner as the changes of the 500 mb surface were determined, provided that we are able to evaluate the right-hand side of the equation. An attempt was next made to test this equation. Maps of the mean height were constructed for the 24th and the 25th of May by means of the following formula, the derivation of which is given in the Appendix:

$$\begin{aligned} z = {} & 0.075\, z_{1000} + 0.15\, z_{850} + 0.175 \\ & z_{700} + 0.2\, z_{500} + 0.15\, z_{300} + 0.1 \\ & z_{200} + 0.15\, z_{100} + 0.05\, T_{1000} + \\ & + 0.06\, T_{700} - 0.24\, T_{300} + 2.68\, T_{100} \qquad (6) \end{aligned}$$

The subscripts denote the pressures to which the heights and temperatures refer. In the computations, T_{1000} and T_{700} were replaced by constant mean values since their variation is seen to be of very little importance. In every gridpoint, the heights and temperatures at the different levels were read from the carefully analyzed constant pressure charts,

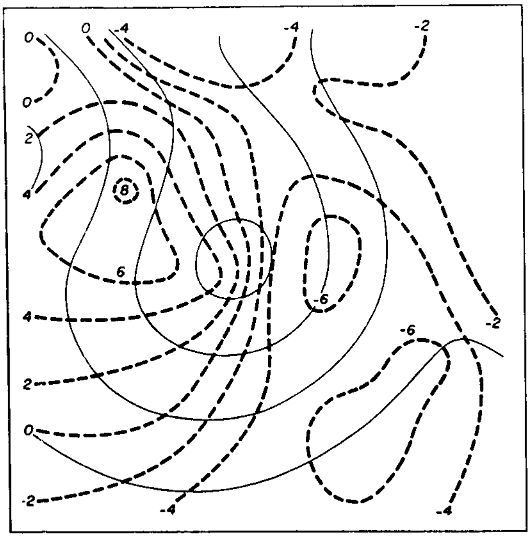

Fig. 7. Observed 12-hour changes in the mean height $\bar{z}$ from 1500 GMT, 24 May to 0300 GMT, 25 May in decameters.

and the mean height was computed. Fig. 5 shows the mean map for the 24th of May at 1500 GMT.

At first, the advection of mean absolute vorticity with the mean wind was determined from the two maps, and a 12-hour height change was computed, disregarding provisionally the last term of (5) and using the same relaxation technique as before. The result is shown in Fig. 6, and the corresponding observed changes of the mean height are shown in Fig. 7. The correlation coefficient between these two change patterns was found to be 0.76. As at the 500 mb level, the computed falls to the SE of the center were too small.

An attempt was then made to include the last term of (5). This may be done under the assumption that the thermal wind $\mathbf{v}_T$ does not change direction with height and that the change in magnitude is similar in all places, so that we may write $\mathbf{v}_T = A_{(p)}\, \mathbf{v}_{T\,1000}$ where $\mathbf{v}_{T\,1000}$ is the surface value of the thermal wind. This is in fact the assumption on which the so-called 2½-dimensional model is based (compare ELIASSEN 1952). Equation (5) may then be written as

$$\frac{\partial \bar{\zeta}}{\partial t} = -\bar{\mathbf{v}} \cdot \nabla (f + \bar{\zeta}) - \overline{A^2}\, \mathbf{v}_{T_{1000}} \cdot \nabla \zeta_{T_{1000}} \qquad (7)$$

The geostrophic value of the surface thermal wind can be determined from the map of $\bar{z}—z_{1000}$ (which is actually a map of the mean temperature since $\bar{z} - z_{1000} = \frac{R}{g} \bar{T}$). We are thus able to evaluate this term under the assumptions mentioned, provided a good estimate can be given to the weighting factor $\overline{A^2}$.

The term was first computed assuming that $A(p)$, is a linear function, so that $\overline{A^2} = 1/3$. The corresponding corrections to the mean height tendencies were again determined by relaxation. The computed 12-hour mean height changes, with this correction included, are shown in Fig. 8. The principal contribution of the thermal wind correction was found to be an increase in the intensity of the area of falls to the S and E of the center, which definitely improved the result. The inclusion of this correction increased the correlation coefficient between observed and computed mean height changes from 0.76 to 0.84.

Actually, the function $A(p)$ deviates considerably from linearity. It has been estimated from a series of ascent curves from Berlin by S. Smebye, and the values are given in an article by ELIASSEN (1952). If these values are used, then the weighting factor $\overline{A^2}$ is found

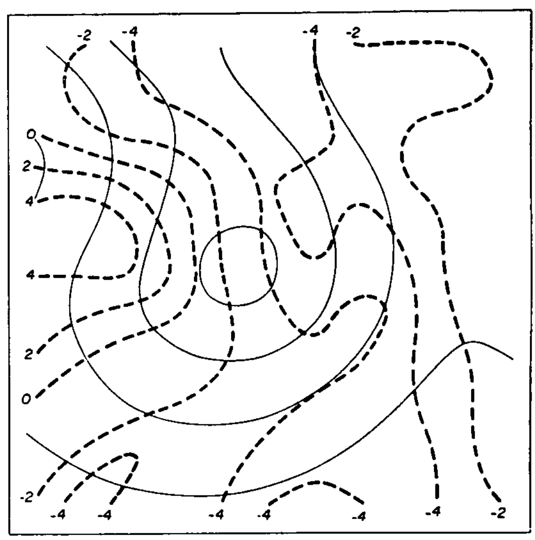

Fig. 8. Computed 12-hour mean height changes from 1500 GMT, 24 May to 0300 GMT, 25 May including thermal wind correction with weighting factor $\overline{A^2} = 1/3$. Units are decameters.

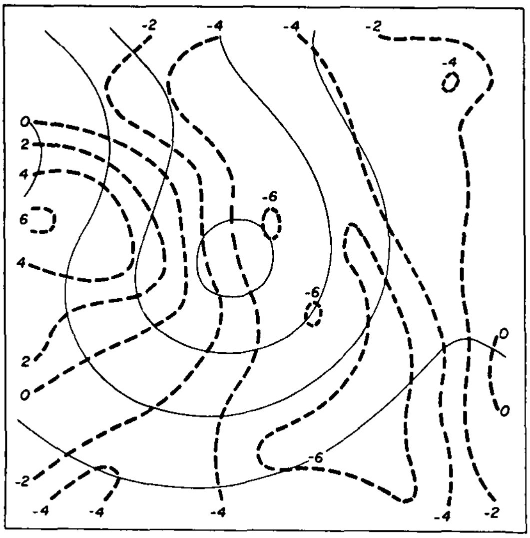

Fig. 9. Computed mean height changes from 1500 GMT, 24 May to 0300 GMT, 25 May including thermal wind correction with weighting factor $\overline{A^2} = 1$. Changes in decameters.

to be closer to unity. When the computations of the 12-hour changes of the mean height were repeated with the values 2/3 and 1 for the weighting factor, the corresponding correlation coefficients between computed and observed changes were 0.86 and 0.89, respectively. Fig. 9 shows the computed changes for $\overline{A^2} = 1$. As far as can be judged from the correlation coefficients, this computation gives a better final result than that based on the 500 mb map. This is confirmed by comparing the computed changes shown in Fig. 9 with the observed changes shown in Fig. 7. Even the falls to the S and E of the center of low pressure show up in the computations with the correct strength. This improvement should not be thought of simply as a result of the inclusion of the thermal wind correction, for the simple barotropic equation crudely incorporates this same term when it is assumed to apply not at the level where $v = \bar{v}$, but rather where $v\,\bar{v} = \overline{v^2}$ (compare CHARNEY, FJØRTOFT and VON NEUMANN 1950). However, when eq. (1) is used, the thermal wind term is assumed to be a constant fraction of the total advection of relative vorticity, whereas it is computed independently using eq. (5).

Making use of the vorticity equation in a diagnostic sense, an attempt was next made to determine the three-dimensional field of motion responsible for the observed vorticity changes. When pressure is used as a vertical coordinate and friction is neglected, the complete vorticity equation may be written (see eq. (5) in ELIASSEN 1952)

$$\frac{\partial \zeta}{\partial t} = -\mathbf{v} \cdot \nabla \eta - \omega \frac{\partial \eta}{\partial p} + \eta \frac{\partial \omega}{\partial p} + \frac{1}{f} \nabla \alpha \cdot \nabla \omega \tag{8}$$

Here p denotes pressure, α specific volume, and ω the individual rate of change of pressure, which is a measure of vertical motion. Moreover, ∇ means here differentiation along an isobaric surface, and $\partial/\partial t$ rate of change in an isobaric surface. Obviously, the local change of vorticity is due partly to advection and partly to non-advective changes represented by the last three terms, which denote vertical transport of vorticity, the effect of horizontal divergence and transformation of horizontal vorticity into vertical vorticity, respectively. The expression for the geostrophic wind has been introduced into the last term. These non-advective vorticity changes are seen to be closely related to the field of ω, i.e. to the vertical motion. In fact, the equation may be used to determine ω when the local and advective changes are evaluated from the synoptic maps. Thus the three non-advective effects may be calculated separately.

The idea to compute the vertical motion from the vorticity equation is not new; similar calculations were made by DEDEBANT and WEHRLE (1933) and by SAWYER (1949).

When ω is considered as the unknown function, eq. (8) is a linear, first-order differential equation. It determines the change of ω along the characteristic lines, which are seen to be the absolute vortex lines. Knowing the distribution of ω over a certain surface, i.e. the earth's surface, the three dimensional field of vertical motion may be determined by integration along the characteristics.

In a barotropic atmosphere $\nabla\alpha = 0$, and the absolute vortex lines are vertical. (Strictly speaking, they are parallel to the earth's axis; the discrepancy, which is unimportant, is introduced by the neglect of the horizontal component of the earth's rotation in the derivation of (8)). The atmosphere is, however, baroclinic in most regions, and the vortex lines are therefore sloping. Generally, the inclination between the vortex lines and the vertical is of minor importance. Strongly baroclinic regions, for example in frontal zones where the absolute vortex lines are roughly parallel to the frontal slope, are an exception. In the situation considered, the slope of the vortex lines was found in most places to be very steep, so that their horizontal projection was much smaller than the grid-size used. It was therefore decided to neglect the slope altogether and to consider the characteristics as vertical. This corresponds to neglecting the term $\frac{1}{f} \nabla \alpha \cdot \nabla \omega$ of eq. (8), which simplifies the computations considerably. Upon doing so, eq. (8) may be written in the form

$$\frac{\partial}{\partial p}\left(\frac{\omega}{\eta}\right) = \frac{\frac{\partial \zeta}{\partial t} + \mathbf{v} \cdot \nabla \eta}{\eta^2} \tag{9}$$

which may immediately be integrated to obtain

$$\left(\frac{\omega}{\eta}\right)_{p=p_1} = \left(\frac{\omega}{\eta}\right)_{p=p_0} - \int_{p_1}^{p_0} \frac{\frac{\partial \zeta}{\partial t} + \mathbf{v} \cdot \nabla \eta}{\eta^2} \, dp \tag{10}$$

Letting p_0 denote the pressure at the ground where the value of ω is known from the kinematical boundary condition, this equation may be used to determine ω at the arbitrary level p_1.

In the computations, the integral in eq. (10) was evaluated by means of the trapezoidal rule from values of $\frac{\partial \zeta}{\partial t} + \mathbf{v} \cdot \nabla \eta$ obtained from analyzed maps of the 1,000, 850, 700, 500 and 300 mb surfaces. For instance, the integral for the layer from 1,000 mb to 850 mb was approximated by

$$\left(\frac{\omega}{\eta}\right)_{850} = \left(\frac{\omega}{\eta}\right)_{1000} - \frac{1}{2}\left[\left(\frac{\frac{\partial \zeta}{\partial t} + \mathbf{v} \cdot \triangle \eta}{\eta^2}\right)_{1000} + \left(\frac{\frac{\partial \zeta}{\partial t} + \mathbf{v} \cdot \triangle \eta}{\eta^2}\right)_{850}\right] 150 \tag{11}$$

and similarly for the other layers. From these expressions, the values of ω were determined at 850, 700, 500 and 300 mb in all gridpoints, assuming $\omega = o$ at 1,000 mb. This is justified because the 1,000 mb surface is close to the ground, and the value of ω at the ground (which is assumed to be level) is much smaller than in the free atmosphere.

The local vorticity changes at the various layers were approximated by the 12-hour change from 1500 GMT the 24th to 0300 GMT the 25th of May. This change may be taken to represent the value of $\frac{\partial \zeta}{\partial t}$ at 2100 GMT on the 24th of May (in the middle of the interval). In order to make the various terms of the equation applicable at the same instant, the vorticity advection must also be determined for the middle instant of the 12 hour interval. Since there are unfortunately no upper air maps available at 2100 GMT, the computation of the vorticity advection was based on mean maps formed by averaging the maps for 1500 GMT and 0300 GMT.

The values of $-\omega$ computed in this way are shown in Figs. 10 a. to 10 d. To a certain extent, the results can be corroborated by comparison with Fig. 11, the surface map for 0000 GMT the 25th of May, which also shows the areas where precipitation was reported during the 12 hour period from 1800 GMT the 24th to 0600 GMT the 25th. The precipitation areas over land are accurate; however, those over water are based on sparse data. The correspondence between the computed vertical motion and the precipitation areas is quite good, and on the whole, the computed vertical motion agrees with what one would expect in such a synoptic situation. The warm front south of Greenland, for instance, is very discernible in the 850 mb vertical motion. Weak descending motion in the warm sector, stronger ascending motion ahead of the front, and descending motion again far ahead of the front (especially at higher levels) all agree with the usual picture. The downward motion to the west of the principal low center and over Norway are also in agreement with reports of clear or partly cloudy skies. The old occlusion across Scotland is likewise illustrated by weak ascending motion associated with reports of light rainfall ahead of it. The correspondence over western France and the

Fig. 10. Twelve hour mean vertical velocity — ω in tens of millibars/6 hours from 1500 GMT, 24 May to 0300 GMT, 25 May at (a) 850 mb, (b) 700 mb, (c) 500 mb and (d) 300 mb. Corresponding mean constant pressure heights shown by thin solid lines.

Bay of Biscay is somewhat poorer. As a whole, the results illustrate the feasibility of computing vertical velocities through the use of the vorticity equation. The computations were here based on observed local vorticity changes; however, if such changes could have been correctly predicted at several levels, the computations of vertical motion could have been based on them as well. Therefore, if we some time in the future will be able to compute satisfactory prognostic maps for several isobaric surfaces, we will also be able to determine the corresponding vertical motion accurately enough to be directly applicable in weather forecasting.

In the 2½-dimensional model, ω is assumed to have a very simple distribution along the vertical, characterized by a maximum value at a certain middle pressure level, and zero values at the top of the atmosphere and at the ground. The computed ω values show very little tendency towards such a simple distribution. However, one cannot draw too definite conclusions from the computations regarding the vertical distribution of ω, because the errors in the computed values must be expected to increase rapidly with height due to doubtful analysis at higher levels. The computed ω values have in some places a maximum as low as 600—700 mb; in other places, no maximum is reached even at 300 mb. The latter is true in several grid points in the area to the SE of the low center. As far as this result can be trusted, it indicates that the level of non-divergence is here actually located above 300 mb, which may explain the poor results of the barotropic tendency computations in this region.

From the computed values of ω, the individual terms of the vorticity equation were evaluated. As one would expect, these terms show quite ragged distributions. In order to reduce these random errors, the values were smoothed by averaging over a square containing nine grid points; the averaged values may be interpreted as circulation changes instead of vorticity changes. The result for the 500 mb surface is shown in figures 12 a to 12 d.

A comparison between these figures shows that horizontal divergence and the vorticity advection seem to be of equal importance in accounting for the local vorticity changes, whereas the vertical vorticity transport seems to be of lesser importance. In fact, the mean absolute values in (6 hours)$^{-1}$/12 hours were 0.221 for $\frac{\partial \zeta}{\partial t}$, 0.125 for $-\mathbf{v} \cdot \nabla \eta$, 0.044 for $-\omega \frac{\partial \eta}{\partial p}$, and 0.175 for $\eta \frac{\partial \omega}{\partial p}$.

In judging these results, however, one should have in mind that the errors resulting from imperfect observations and analysis, as well as from the geostrophic wind approximation will tend to increase the absolute magnitudes of the computed values of ω and the divergence term. The mean absolute values for $-\omega \frac{\partial \eta}{\partial p}$ and $\eta \frac{\partial \omega}{\partial p}$, given above, are therefore likely to be overestimates.

To the W of the low center, the advection seems to account for the greater part of the local vorticity decrease observed in this region, but the local vorticity increase observed SE and E of the center must be almost entirely ascribed to the effect of horizontal convergence. Therefore as far as the calculations can

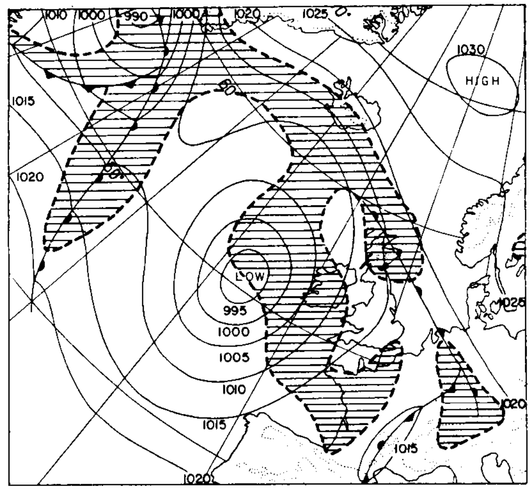

Fig. 11. Surface map for 0000 GMT, 25 May showing reported precipitation areas during the period from 1800 GMT, 24 May to 0600 GMT, 25 May.

be trusted, the indications are that the vorticity increase necessary to keep the field of motion semi-stationary is produced by this horizontal convergence.

Appendix.

The mean height $\bar{z}$ is defined as

$$\bar{z} = \frac{1}{p_0} \int_0^{p_0} z \, dp \tag{12}$$

where p_0 is put equal to 1,000 mb. Integrating by parts, and using the hydrostatic equation, this equation may be written

$$\bar{z} = z_{1000} + \frac{R}{g} \frac{1}{p_0} \int_0^{p_0} T \, dp \tag{13}$$

Thus $\bar{z}$ may be determined simply by graphical integration of the ascent curve, plotted in a pT-diagram.

However, if the values of z and T at several isobaric levels are already known, we may to a certain extent utilize this information, and thereby save work.

Suppose that we know from the aerological report that the isobaric surface p_0 has the height z_0 and the temperature T_0; the isobaric surface p_1 has the height z_1 and temperature T_1, and

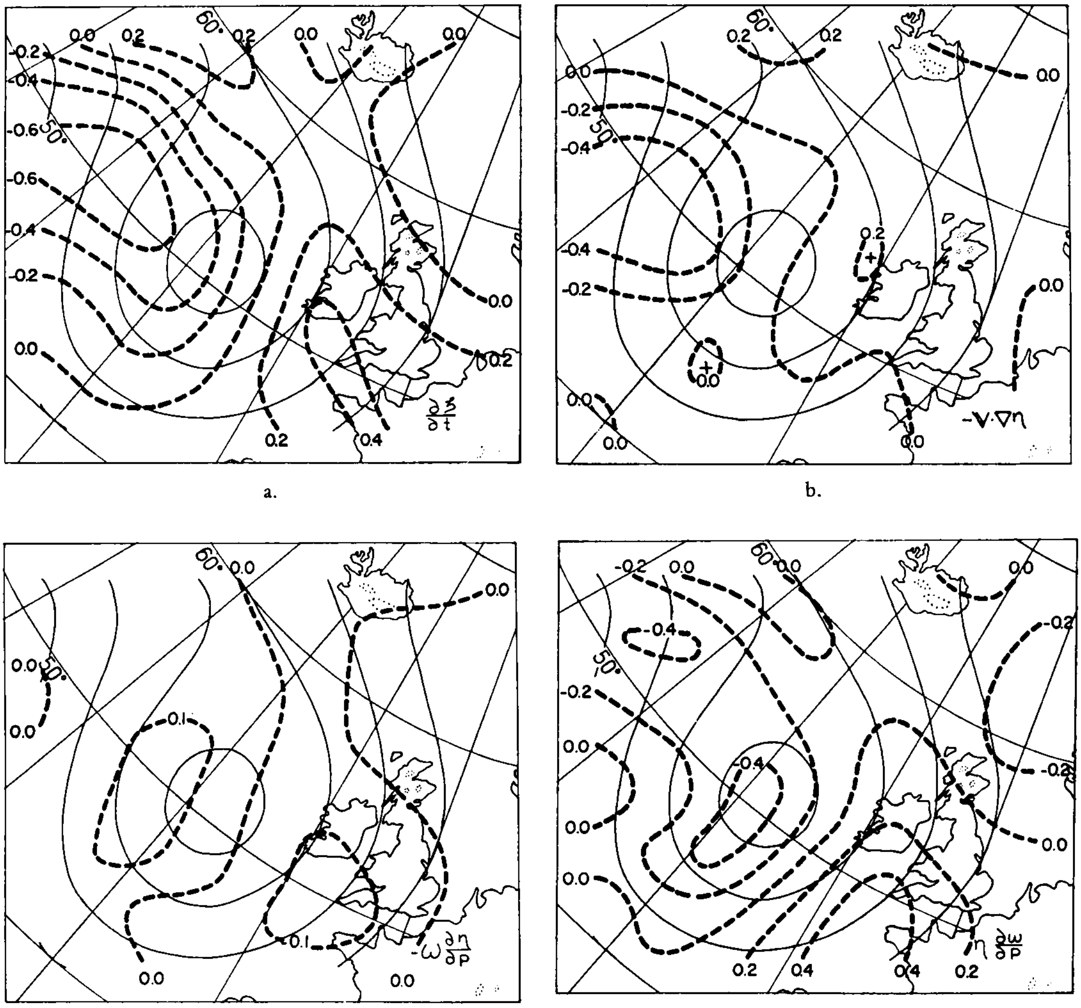

Fig. 12. Smoothed values of (a) $\frac{\partial \zeta}{\partial t}$, (b) $-\mathbf{v} \cdot \nabla \eta$, (c) $-\omega \frac{\partial \eta}{\partial p}$ and (d) $\eta \frac{\partial \omega}{\partial p}$ at 500 mb obtained by averaging over nine gridpoints. Units (6 hours)$^{-1}$/12 hours. Mean 500 mb pattern shown by thin solid lines.

so on. The integral in (13) is then broken up into a sum of integrals over the layers between these levels. Consider one of these integrals, over the layer from p_0 to p_1. Within this layer, we approximate z by a polynomial in p of the third degree,

$$z(p) = A + Bp + Cp^2 + Dp^3 \qquad (14)$$

where A, B, C and D are constants. This function must satisfy the four conditions

$$\begin{aligned} z\ (p_0) &= z_0 \\ z\ (p_1) &= z_1 \\ z'\ (p_0) &= -\frac{R\ T_0}{g\ p_0} \\ z'\ (p_1) &= -\frac{R T_1}{g\ p_1} \end{aligned} \qquad (15)$$

These equations determine the values of A, B, C and D. When the values of the coefficients thus obtained are introduced into (14), and the integration is carried out, we obtain

$$\int_{p_1}^{p_0} z\,dp = A\,(p_0 - p_1) + \frac{1}{2}\,B\,(p_0^2 - p_1^2) + $$
$$+ \frac{1}{3}\,C\,(p_0^3 - p_1^3) + \frac{1}{4}\,D\,(p_0^4 - p_1^4) =$$
$$= \frac{z_0 + z_1}{2}\,(p_0 - p_1) -$$
$$- \frac{1}{12}\frac{R}{g}\,(p_0 - p_1)^2\left(\frac{T_1}{p_1} - \frac{T_0}{p_0}\right) \qquad (16)$$

This formula was applied to the layers 1,000—850 mb, 850—700 mb, 700—500 mb, 500—300 mb, 300—200 mb and 200—100 mb. Clearly, the same formula does not work for the uppermost layer, 100—0 mb. For this layer it was instead assumed that the temperature is constant and equal to T_{100}; this gives

$$\int_0^{100} z\,dp = \left(z_{100} + \frac{R}{g}\,T_{100}\right)\ 100\text{ mb} \qquad (17)$$

When the integrals are added, we finally obtain

$$\bar{z} = 0.075\,z_{1000} + 0.15\,z_{850} + 0.175 z_{700} +$$
$$0.2\,z_{500} + 0.15\,z_{300} + 0.10\,z_{200} + 0.15\,z_{100} +$$
$$+ \frac{R}{g}\,(0.00188\ T_{1000} + 0.00208\ T_{700} -$$
$$- 0.00833\ T_{300} + 0.09167\ T_{100}) \qquad (18)$$

which is identical with (6).

REFERENCES

BOLIN, B. and CHARNEY, J. G., 1951: Numerical Tendency Computations from the Barotropic Vorticity Equation. *Tellus*, **3**, pp. 248—257.

CHARNEY, J. G., 1949: On a Physical Basis for Numerical Prediction of Large-Scale Motions in the Atmosphere. *J. Meteor.*, **6**, pp. 371—385.

CHARNEY, J. G., FJÖRTOFT, R. and VON NEUMANN, J., 1950: Numerical Integration of the Barotropic Vorticity Equation. *Tellus*, **2**, pp. 237—254.

CRAIG, R. A., 1945: A Solution of the Nonlinear Vorticity Equation for Atmospheric Motion. *J. Meteor.*, **2**, pp. 175—178.

DEDEBANT, G. and WEHRLÉ, PH., 1933: L'équation du Tourbillon Synoptique et son Application à la Théorie du Système Nuageux. *U. G. G. I. Cinquième Assemblée Générale.* Lisbonne 1933. *Proc. Verb. de L'A. I. M.* **2**, pp. 117—144.

ELIASSEN, A., 1952: Simplified Dynamic Models of the Atmosphere Designed for the Purpose of Numerical Weather Prediction. *Tellus*, **4**, pp. 145—156.

HÖILAND, E., 1950: On Horizontal Motion in a Rotating Fluid. *Geof. Publ.* **17**, No. 10, pp. 5—26.

SAWYER, J. S., 1949: Large Scale Vertical Motion in the Atmosphere. *Quart. Jour. R. M. S.* **75**, pp. 185.

Staff Members, University of Stockholm, 1952: Preliminary Report on the Prognostic Value of Barotropic Models in the Forecasting of 500 mb Height Changes. *Tellus*, **4**, pp. 21—30.